communications earth & environment

Article

https://doi.org/10.1038/s43247-024-01855-0

Salt marsh litter decomposition varies more by litter type than by extent of sea-level inundation

Marie Arnaud[1,2,3] ✉, Melissa Bakhos[3], Cornelia Rumpel[3], Marie-France Dignac[3], Nicolas Bottinelli[3], Richard J. Norby[2,4], Philippe Geairon[1], Jonathan Deborde[1], Pierre Kostyrka[1], Julien Gernigon[5], Jean-Christophe Lemesle[5] & Pierre Polsenaere[1]

Salt marshes are among the most efficient blue carbon sinks worldwide. The fate of this carbon is uncertain due to limited knowledge about organic matter (OM) decomposition processes under sea-level rise. In an in-situ manipulative experiment, we compared salt marsh OM decomposition and quality across simulated sea-level scenarios (by modifying the inundation) and litter types (absorptive root, fine transportive root, leaves, and rhizomes of *Halimione portulacoide*) for 170 days. The litter decomposition varied only between the inundation treatments with the longest and shortest durations, while the decomposition differed significantly across litter types, with absorptive roots releasing up to 40% less carbon than other litters. Changes in lignin composition were minimal for absorptive roots and were unaffected by sea-level rise scenarios. Our study suggests that (i) current projections of sea-level rise are unlikely to decrease litter decomposition; (ii) separating litter types might lead to better assessments of salt marshes' OM dynamics.

Salt marshes are part of blue carbon (C) ecosystems[1], holding up to 1350 Tg C[2]. Each year, they bury ~200 g C m^{-2}, which is one order of magnitude greater than terrestrial forests[1]. A salt marsh C sink is largely a balance between primary production and the decomposition of autochthonous plant litters, as well as the inputs of C from allochthonous sources (especially in mineral salt marshes)[3,4]. Those processes strongly depend on environmental conditions, e.g., inundation duration[5]. It has not yet been fully resolved as to whether salt marshes will continue to act equally as a C sink and store following accelerated sea-level rise (SLR) and climate change[5–8]. SLR might increase the inundation duration and frequency, as well as induce coastal erosion[9]. Inundation might reduce OM degradation due to oxygen limitations, higher sulphate availability or changes in plant root activity[10–15]. Yet, in salt marshes and mangroves, a decrease in inundation duration had contrasting impacts on the belowground organic matter (OM) decomposition rate, with varying results: either a drastic increase (up to tenfold[12,13]), no effect at all or a decrease in the belowground OM decomposition[14,16–18]. Thus, the effect of inundation can vary and is probably influenced by the chemical composition of the OM types deposited in these environments.

Decomposition rates and their controls are currently drawn mostly from aboveground litter in coastal wetlands[19]. Yet, root may be a major source of OM (up to 70%) accumulated in salt marshes[4]. To the best of our knowledge, there are no biomass estimates for the various root functional types for salt marshes, likely because the root dynamics (production, decomposition, mortality) have not been considered to be different across root functional types. However, belowground material such as rhizomes, fine absorptive and fine transportive roots might have contrasting decomposition rates in salt marshes, as observed across terrestrial ecosystems and mangroves[20–22]. These types of OM may have a contrasting composition due to functional differences. For example, the finest distal roots (order 1-2-3) absorb water and nutrients, and fine roots of higher orders (order 4) transport those components[20]. Like leaves, fine absorptive roots (order 1-2-3) have a relatively low carbon-to-nitrogen (C:N) ratio and were previously thought to decompose faster than fine transportive roots in terrestrial ecosystems[23]. However, studies from terrestrial and mangrove ecosystems have shown that fine absorptive roots were the slowest to decompose[21,24–26]. These results highlight the need for a better understanding of the decomposition dynamics across plant tissues in salt marshes, especially under accelerated SLR scenarios.

The decomposition rates of litter in coastal wetlands are often forecasted using the C:N ratio or N content of the litter. The loss of

[1]Ifremer, LITTORAL, La Tremblade, France. [2]School of Geography, Earth and Environmental Sciences, University of Birmingham, Edgbaston, Birmingham, UK. [3]CNRS, Sorbonne Université, INRAE, IRD, Institut of Ecology and Environmental Sciences (IEES), Paris, France. [4]Department of Ecology and Evolutionary Biology, University of Tennessee, Knoxville, TN, USA. [5]Réserve naturelle nationale de Lilleau des Niges & Ligue pour la protection des oiseaux, Les Portes en Ré, France. ✉e-mail: m.arnaudd@gmail.com

both C and N is also widely reported after decomposition, and analyses of stable isotope composition and lignin ratios (lignin-to-polysaccharide (LigPS) and lignin monomer ratios) are emerging as valuables approaches to assess the degree of plant material decomposition[27–31]. In particular, the evaluation of lignin ratios has been used to assess soil OM degradation in coastal wetlands[32]. This method hinges on the differential degradation rates of the various lignin types. The use of different lignin monomers has also proven effective in evaluating the decomposition of bulk soil OM, given the discernible selective degradation of the syringyl units (monomer: LigS) in contrast to the guaiacyl units (monomer: LigG) during the decomposition of OM in coastal wetland soils[32]. These ratios can be supplemented by measurements of the detrital stable C and N isotope signatures. While some research has shown minimal isotopic fractionation during decomposition (<1‰ over 28–168 days), others have demonstrated more pronounced variations (>4‰) in $\delta^{15}N$ and/or $\delta^{13}C$[27–30]. These contrasting outcomes underscore the critical need for an enhanced understanding of the complex interplay between plant decomposition dynamics, as well as isotope signatures and lignin ratios across environmental conditions in diverse coastal ecosystems.

We focused on the impact of accelerated SLR represented by the inundation duration and frequency on the decomposition of leaf litter and contrasting root functional types, which are the main contributors to blue carbon accumulating in salt marshes[4]. To this end, we conducted an in-situ mesocosm experiment with five different levels of inundation to investigate the degradation of different plant tissue types (hereafter referred to as litter type) under contrasting inundation levels. We used plant tissues of the shrubby C_3 halophyte *Halimione portulacoides* (L. Allen, also named *Atriplex portulacoides*), which is widespread on salt marshes along the coasts of Europe, North Africa and South-West Asia[33], but which has received relatively little attention compared to species from the *Spartina* genus[19]. Leaves, two functional root types, and rhizomes were exposed in litterbags for 170 days.

We had three research questions:

1. How do changes in inundation (associated with SLR) affect the decomposition rates of leaves, fine absorptive roots, fine transportive roots and rhizomes?
2. Do the decomposition rates differ among leaves, fine absorptive roots, fine transportive roots and rhizomes?
3. How do the litter types and inundation modify the loss of C and N, as well as the chemical and isotopic composition of the decomposing plant-derived OM?

Here, we show that leaves decompose faster than roots, and that fine absorptive roots decompose the slowest. We further show that inundation and litter types did not interact to control the decomposition rate and chemical composition of the plant-derived OM. For the comparison of litter types mass loss and chemistry, we used a recommended pooling method[34] to avoid bias due to plant location, which might have reduced the variability between replicate of each litter type. As we intended to test the influence of the edaphic environment (inundation), the incubated litter should be as homogenous as possible.

Results

Environmental conditions and litter chemistry before exposure

Large variations in the environmental conditions were measured across our inundation treatments (Table 1). The shortest inundation duration (2% and 0.5 h d^{-1} for SL-40) was 1/20th the size of the largest one (43% and 10.3 h d^{-1} for SLR100) during the measurement period (Table 1). The C content was similar across the root and rhizome litters, ranging between 43.5% in fine absorptive roots and 45.5% in rhizomes and was the lowest in leaves (31.3%) (Table 2). The highest N concentration was recorded for fine absorptive roots (1.80%), followed by fine transportive roots (1.69%), leaves (1.41%) and rhizomes (0.87%, Table 2). The initial C:N ratio was the lowest in leaves (22.3) and fine absorptive roots (24.2), followed by fine transportive roots (26.0) and rhizomes (52.4, Table 2). The $\delta^{13}C$ value ranged from −26 to −25.3‰, and $\delta^{15}N$ was between 4.8 and 10. 3‰, with the most enriched $\delta^{13}C$ in leaves and the most depleted $\delta^{13}C$ in fine transportive roots. The Lig:PS proxy was approximately 2.5 times higher in rhizomes (2.66) than in fine absorptive roots (1.07) and roughly 1.5 times lower in fine transportive roots than in rhizomes (1.61, Table 2). The LigG:LigS proxy was the highest in fine absorptive roots (2.09), followed by fine transportive roots and rhizomes (Table 2). The lignin proxies were not calculated for the leaves because their lignin content was too low.

Table 1 | Environmental conditions across our inundation treatments from the least inundated (SL-40) to the most inundated (SLR100)

	Volumetric water content[a] (%)	Inundation duration[b] (%)	Inundation duration[2] (h d^{-1})
SL-40	44.3	2	0.5
SLI	50.1	8	1.8
SLR30	51.8	14	3.4
SLR60	52.2	22	5.4
SLR100	53	43	10.3

SLI is the mean altitude of our site. SLR30 is the simulated SLR under SSP1−2.6. SLI60 is the simulated SLR under SSP3-7. SLR100 is the simulated SLR above predictions, and SL-40 represents a lower level of inundation than the mean inundation of our site. Please see Methods section for more information.

[a]measured on four random dates across all mesocosms and measured as volumetric water content in a cylinder of sediment of 3 cm in diameter and 6 cm in length, $n = 100$.

[b]measured at the marsh organ between May 4, 2021 and October 20, 2021. h d^{-1} is hour per day.

Mass loss across treatments

During the experiment, the mass loss ranged from 22% to 52%. Based on pooled samples, the mass loss was significantly different across the litter types ($P < 0.001$; Fig. 1; Table 3). Fine absorptive roots had the lowest median mass loss (22%), followed by rhizomes (24%), fine transportive roots (30%) and leaves (52%) (Supplementary Table 1). Fine absorptive roots decomposed ~60% slower than leaves ($P < 0.001$), ~30% slower than fine transportive roots ($P < 0.001$), and ~10% slower than rhizomes ($P = 0.002$), based on pooled samples. The litter decomposition rate was significantly different only between the longest (SLR100) and shortest inundation duration (SL-40) ($P < 0.01$; Table 3). All of the other inundation treatments were not statistically different (all pairs of samples $P > 0.05$; Table 3). The longest inundation duration treatment (SLR100) had the lowest mass loss (24 %; Supplementary Table 1). The shortest inundation duration treatment (SL-40) had the highest mass loss (31%) (Supplementary Table 1). The litter types and inundation treatment did not interact significantly to affect the litter decomposition rate ($P = 0.85$; Table 3). When treated as a continuous variable, the inundation treatment (as h d^{-1}) was not linearly related to the mass loss ($r^2 = 0.005$; $p = 0.5$).

Products and proxies from the pyrolysis analysis

We identified several pyrolysis products in all the litter types, originating from lignin, lipids, polysaccharides and N-containing compounds (Supplementary Table 2). The data are based on triplicate analyses of each pooled sample of the litter type, which might have reduced the variability within each litter type.

The principal component analysis (PCA) of the relative areas obtained with pyrolysis-GC/MS revealed two distinct groups of pyrolysis products: A and B. Group A products originated from lipids (aliphatics) and group B originated from lignin-derived products (LigG, LigS), polysaccharide-derived products and non-specific phenols. There was a good discrimination between the leaves (on the left) and the roots/rhizomes litter (on the right) on the two first axes of the PCA. The leaves were correlated with the group A pyrolysis products, indicating high contents and proportions of aliphatics compared to the other samples. The roots/rhizomes were correlated to the group B products, indicating a mixture of molecules, including lignin G, lignin S, polysaccharides, N-containing compounds and phenols.

Table 2 | Initial elemental content and chemical decomposition indicators across the root functional types before field exposure of *Halimione portulacoides*

	C (%)	N (%)	C:N	$\delta^{13}C$ (‰)	$\delta^{15}N$ (‰)	Lig:PS proxy	LigG:LigS proxy
Fine absorptive roots	43.5	1.80	24.2	−25.7	6.3	2.09	1.07
Fine transportive roots	44.0	1.69	26.0	−26	4.8	1.32	1.61
Rhizomes	45.5	0.87	52.4	−25.6	8.1	0.68	2.66
Leaves	31.3	1.41	22.3	−25.3	10.3	n.a	n.a

The data are based on triplicate analyses of each pooled sample of the litter type, which might have reduced the variability within each litter type and precluded firm conclusions about the results. C is the carbon concentration, N is the nitrogen concentration, LigG:LigS is the ratio of guaiacyl lignin on syringyl, and Lig:PS is the ratio of total lignin on polysaccharide calculated with the pyrolysis. All are expressed as the mean for LigG:LigS and Lig:PS only. Leaves had too little lignin, and therefore the LigG:LigS and Lig:PS ratio could not be calculated.

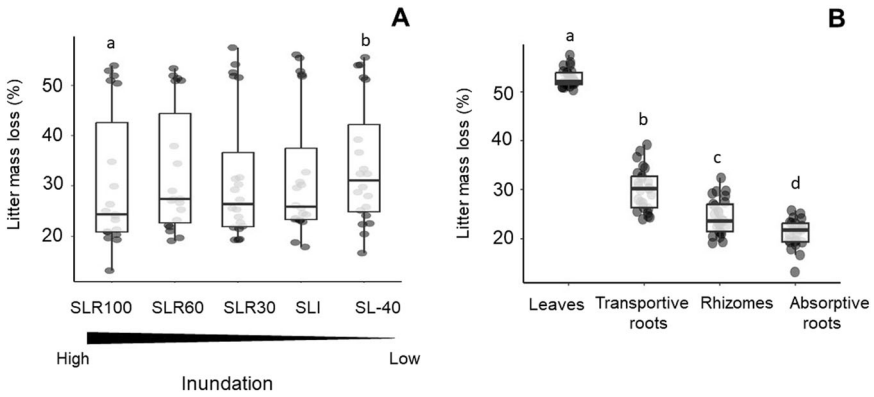

Fig. 1 | Response of the litter mass loss of *Halimione portulacoides* to inundation regimes and litter types. Response of the litter mass loss (%) to inundation regimes (**A**) and litter types (**B**) for *Halimione portulacoides* over the 170-day measurement period. SLR100 was the most inundated treatment, SLI was the initial inundation condition and SL-40 was the least inundated, see Table 1. Thick bars indicate the sample medians; the box ends indicate the upper and lower quartiles; the box whiskers extend to the maxima and minima of each sample (excluding the outliers). Circles indicate individual measurements. Only significant ($P < 0.05$) differences between the treatments are displayed, and different letters are used for each treatment (Table 3). The litter mass loss for each litter type is based on pooled litters from different locations, which might have reduced the variability across replicates.

Table 3 | Statistical results on the percentage change mass, carbon and nitrogen masses, as well as percentage change in $\delta^{13}C$, $\delta^{15}N$ and both lignin ratios across the litter types and degree of inundation

	Mass loss	C	N	$\delta^{13}C$	$\delta^{15}N$	Lig:PS proxy	LigG:LigS proxy
OM type	<0.01	<0.01	<0.01	<0.01	0.1	<0.01	<0.01
Inund.	0.02	<0.01	<0.01	0.19	0.64	0.27	0.68
OM:Inund.	0.85	0.36	0.7	0.78	0.95	na	na
Pairwise comparison between litter types	$P < 0.05$ for all combination	$P < 0.05$ for all combinations, except RZ vs RA; RT vs L	$P < 0.05$ for all combinations, except RZ vs RA; RT vs L	$P < 0.05$ for L vs. RA; L vs RT; L vs RZ	na	$P < 0.05$ for all combinati-on	$P < 0.05$ for RT vs. RA; RZ vs RT
Pairwise comparison between inundation	$P < 0.05$ for combination SLR100 vs. SLI-40	$P < 0.05$ for combination SLR30 vs SLI and SLR30 vs. SLI-40	$P < 0.05$ for combination SLI-40 vs SLR100, SLI-40 vs SLR60 and SLI-40 vs. SLR30	na	na	na	na

The effects of litter types, inundation treatment and their interaction for the other variables (C, N, δ13C, δ15N, Lig:PS, LigS:LigG) were analysed using Kruskal-Wallis tests. Post-hoc pairwise comparisons were conducted using Dunn tests. SLR100 was the most inundated treatment, SLI was the initial inundation condition and SL-40 was the least inundated treatment, see section Materials and Methods 2.1. For all variables, $n = 60$, except for mass loss ($n = 100$) and for Lig:PS and LigG:LigS ($n = 45$). Inund is the inundation treatment, C is carbon, N is nitrogen, Lig:PS is the lignin-to-polysaccharide ratio, LigG:LigS is the ratio between the guaiacyl units/syringyl units, RA stands for fine absorptive roots; RT indicates fine transportive roots; RZ stands for rhizomes; L stands for leaves. Refer to Table 1 for the level of inundation. The statistical results per litter type are based on replicate made of pooled litters from different locations, which might have reduced the variability across the replicates.

Change of elemental composition, stable C and N isotope composition, and lignin ratios

The changes in C and N mass, and in the $\delta^{13}C$, $\delta^{15}N$ and lignin parameters during decomposition, were mostly different across the litter types ($P < 0.01$, except for $\delta^{15}N$; Table 3, based on pooled litters from different locations that might have reduced the variability across replicates), but mostly similar across the inundation gradient. There was no significant interactive effect between the litter types and inundation gradient for any of the parameters mentioned above (all $P > 0.36$). Hereafter, we report the median value between the initial and litter exposed for 170 d for all chemical and isotopic variables. Highest C and N mass loss was recorded for leaves ($C = 29\%$; $N = 48\%$), while fine absorptive roots showed the lowest loss. Fine absorptive roots showed 50% less C loss, and 65% less N loss than leaves (Supplementary Table 1; Fig. 2). The differences in the C and N mass changes were significant between (i) leaves and fine absorptive roots, (ii) leaves and rhizomes, and (iii) fine absorptive roots and transportive roots, which lost 36% less C and 60% less N than absorptive roots (all $P < 0.01$; Table 3; Fig. 2; based on pooled samples). The percent change in $\delta^{13}C$, Lig:PS and LigG:LigS

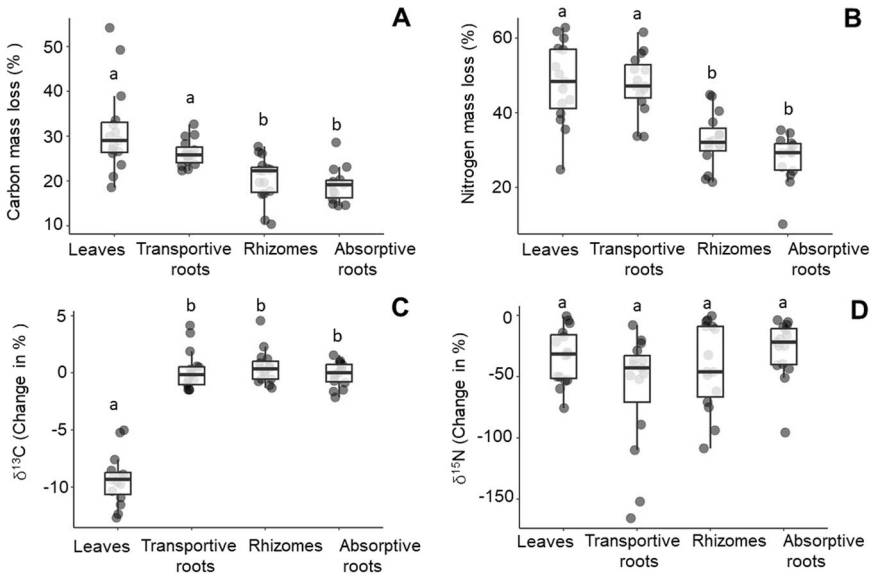

Fig. 2 | Carbon and Nitrogen mass loss, as well as the change in $\delta^{13}C$ and $\delta^{15}N$ across the litter types of *Halimione portulacoides*. Carbon (**A**) and Nitrogen (**B**) mass loss (in %), as well as the change in $\delta^{13}C$ (**C**) and $\delta^{15}N$ (**D**) across the litter types for *Halimione portulacoides* over the 170-day measurement period. Thick bars indicate the sample medians; the box ends indicate the upper and lower quartiles; the box whiskers extend to the maxima and minima of each sample (excluding outliers). Circles indicate individual measurements. For the significant ($P < 0.05$) differences between the treatments, refer to Table 3. The chemistry results for each litter type are based on pooled litters from different locations, which might have reduced the variability across replicates.

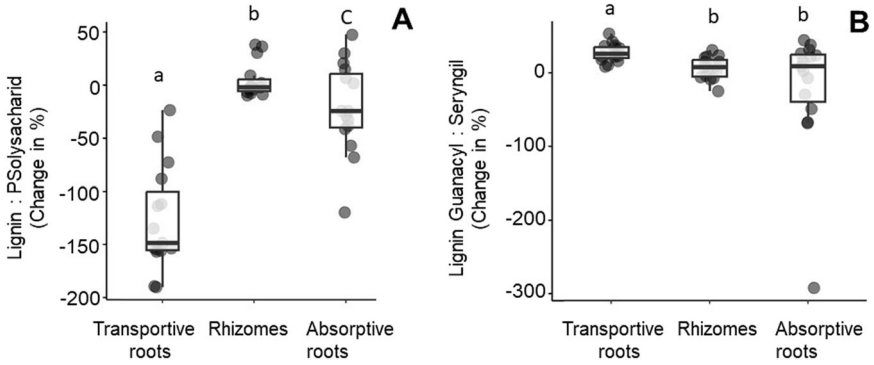

Fig. 3 | Changes in the lignin-to-polysaccharide ratio and lignin guaiacyl-to-syringyl ratio across the litter types for *Halimione portulacoides*. Changes (%) in the lignin-to-polysaccharide ratio (**A**) and lignin guaiacyl-to-syringyl ratio (**B**) across the litter types for *Halimione portulacoides* over the 170-day measurement period. Thick bars indicate the sample medians; the box ends indicate the upper and lower quartiles; the box whiskers extend to the maxima and minima of each sample (excluding outliers). Circles indicate individual measurements. For significant ($P < 0.05$) differences between the treatments, refer to Table 3. Note that both ratios are proxies that have been calculated from the pyrolysis products. The chemistry results for each litter type are based on pooled litters from different locations, which might have reduced the variability across replicates.

between the initial and exposed litter varied across the litter types (all $P < 0.01$), but not across the inundation gradient (all $P > 0.27$; Table 3; Fig. 2).

Indeed, the percentage change in $\delta^{13}C$ value decreased by 9% for the leaves but varied by less than 0.3% for the other litter types. The percentage change in $\delta^{13}C$ was significant only between the leaves and the other litter types ($P < 0.05$; Table 3). The percentage change in $\delta^{15}N$ did not differ significantly across the litter types ($P = 0.1$). The change of Lig:PS between the initial and exposed litter was different across all belowground litter types ($P < 0.05$) and ranged between −148% for fine transportive roots, −24% for fine absorptive roots and −2% for rhizomes (Supplementary Table 1; Fig. 3). The difference in LigG:LigS between the initial and exposed litter varied significantly across the litter types ($P < 0.05$) ranging from 26% for fine transportive roots, 9% for fine absorptive roots and 7% for rhizomes. Yet, only the fine transportive roots were different from other litter types for LigG:LigS ($P < 0.05$). The difference in LigG:LigS between the initial and exposed litter was not significant across the inundation treatments ($P = 0.68$; Table 3).

Discussion

Effect of litter type on the belowground OM decomposition rates

Our results indicated that leaves decomposed the fastest, whereas fine absorptive roots exhibited the slowest decomposition, consistent with the findings reported for terrestrial woody plants and mangroves[21,25,26,35]. Fine absorptive roots have been shown to decompose up to three times slower than leaves[25], and from 10 to 150% slower than fine transportive roots depending on the species and incubation times[26,36]. Thus, the difference in decomposition between fine absorptive and fine transportive roots in our experiment (30%) is within the range of the few reported values[24,36,37]. Our results showed that the decomposition rate of fine absorptive roots (~21% mass loss) and fine transport roots (30% mass loss) fell within the range of values reported for a mangrove, where fine absorptive roots lost 16 to 23% of their mass after 183 days, while fine transportive roots lost 22–33% of their mass after 183 days[26]. Similar results were also recorded in terrestrial forests[24,36,37]. We could not compare our results to other salt marshes, because to our knowledge there are no other studies on root decomposition across functional type. Our results are nevertheless in accordance with previous findings showing that the above-ground organs of salt marsh plants decay faster than bulk roots[38]. Our data indicate that the litter types strongly controlled the OM decomposition rates, most probably due to their contrasting chemical composition. Traditionally, C:N ratios and N concentrations were used to predict the aboveground OM decomposition rate[23] and are believed to control OM decomposition in salt marshes[16]. Yet, our study showed that fine absorptive roots had a low C:N ratio and a high N content like leaves but decomposed the slowest. The slower decomposition of fine absorptive roots compared to leaves could be attributed to the (high) lignin content of roots[38], which is known to be more recalcitrant and difficult

to decompose under anaerobic conditions[35], whereas leaves are almost lignin free. The lipids are believed to be more preserved than lignin under anaerobic conditions[39], which contrasts with our finding that leaves decomposed the fastest, despite being mostly composed of lipids. Our results indicated contradictory results as the highest lignin/polysaccharide (Lig:PS proxy) ratio was recorded for rhizomes, followed by fine transportive roots and fine absorptive roots, although transportive roots showed the highest degradation rate. These differences might be related to the lignin composition, as the guaiacyl/syringyl lignin ratio (LigG:LigS proxy) was associated with the lower decomposition rate of fine absorptive roots compared to rhizomes and fine transportive roots. Fine absorptive roots showed the highest LigG:LigS proxy indicating a higher proportion of more stable guaiacyl units. Guaiacyl lignin has been shown to degrade more slowly than syringyl lignin due to its higher proportion of resistant dimer C-C bindings and to its localization in the inner part of the lignin structure[40]. Our results are in agreement with previous studies in terrestrial environments showing that the chemical composition of lignin might be a more robust predictor of OM decomposition rates than total lignin[41].

Molecular composition, isotopic ratio and lignin ratio changes after exposure

The loss of C and N relative to their initial masses were the highest in leaves and fine transportive roots, and lowest in fine absorptive roots. Our results contrast with the assumption that (1) leaf decomposition can be extrapolated for all litter types in blue C ecosystems[19], and (2) belowground litter represents a homogeneous group for decomposition studies in salt marshes. The differences between fine absorptive roots, leaves and fine transportive roots are similar to those reported in terrestrial ecosystems[25,37], and suggest that a similar pattern may occur, as observed in other blue C ecosystems, such as mangroves[26].This implies that extrapolating litter decomposition from one single type of litter, often done with leaves as they are easier to collect, might not be representative of the overall bulk soil litter decomposition. Therefore, to accurately quantify the litter inputs to humus that are part of the soil C stock, each litter type's production, mortality, and decomposition should be quantified.

The Lig:PS proxy strongly increased upon the decomposition of fine transportive roots and, to a lesser extent, of rhizome and fine absorptive roots. This indicates an increase in the lignin concentration of the litter during decomposition, consistent with findings for litter decomposition in terrestrial environments[31]. We also found a marked depletion in $\delta^{13}C$ for leaves, indicating large plant tissue degradation, as previously observed[28], but no shift for the other litter types. This was in accordance with our results showing that leaves had the highest decomposition rate and fine absorptive and fine transportive roots had the highest increase in the Lig:PS ratio. Labile compounds, such as polysaccharides, are enriched in ^{13}C while lignins are depleted[29]. Therefore, an increase in the Lig:PS ratio should correspond to an ^{13}C enrichment of the $\delta^{13}C$. Indeed, $\delta^{13}C$ was well correlated to the decomposition rate, in contrast to $\delta^{15}N$, where no clear shift occurred across all our litter types, as previously reported[28].

It is worthwhile to note that our findings on litter mass loss and chemistry across different types of litter, as well as findings from other studies, are often based on replicates made from pooled litters from different individuals. The use of standardized or pooled litter has been recommended to limit any bias due to litter quality as confounding factor[34,42].

Effect of inundation on the belowground OM decomposition rate

The effect of inundation on OM decomposition in our marsh organ experiment was small (Fig. 1) and similar to what has been previously reported in other salt marshes[16,17,43,44]. We observed a slight significant increase in the OM decomposition rate with a decrease in the inundation duration, which was only statistically significant between the most and least inundated treatments (Fig. 1, Table 3). The increase in the OM decomposition rate in the least inundated treatment might be linked to a longer exposure of the soil surface to the atmosphere[45,46] since this treatment was inundated only during the spring tide. It is interesting to note that the mean inundation levels did not show any significant differences with the extreme treatments, indicating that the predicted accelerated SLR scenarios under those conditions might not affect the decomposition of litters. The predicted accelerated SLR might nevertheless induce a loss of OM through indirect effect, such as salt marsh sediment losses by erosion, which could otherwise retain OM[9]. The effect of inundation on the decomposition rate was similar across the root functional types, which were found to be almost insensitive to the inundation duration, as observed in a mangrove[26]. Our results imply that, with predicted SLR, elevation gain through carbon accrual[7] is unlikely due to a lack of modified rates of litter decomposition. A potential elevation gain and resistance of the studied salt marsh to SLR may therefore be restricted to other factors, such as an increase of sediment accretion, or to factors leading to an increase in organic matter accumulation, such as an increase in root production and life-expectancy, or a shift of C allocation to root functional types decomposing at a slower rate (i.e., fine absorptive roots)[47–49]. If mangroves allocate more carbon to fine absorptive roots, these roots will constitute a larger proportion of the total litter. Since fine absorptive roots decay slowly, their relative dominance in the litter will result in a slower overall decay rate, regardless of the level of inundation. Organic salt marsh sediments include a large portion of dead root materials; therefore, an alteration of root production and decomposition will disproportionally modify their soil surface elevations and resilience to SLR[50]. In salt marshes with more mineral soils, like in our site, the current elevation change is dominated by sediment inputs[51], but a change in soil surface elevation might occur if root production and decay are altered, notably under global changes[52], such accelerated SLR[48,53].

Implications for carbon budgets

The litter decomposition rate and its control in blue C ecosystems are often extrapolated from leaves to all litter types[19]. Global decomposition rate of salt marsh litters have been recently estimated to be $5.9 \pm 0.5 \times 10^{-3}$ d^{-1} using exclusively leaf litter measurements[19]. If we assume equal inputs of all litter types to the soil, using only the decomposition rate of leaves would artificially inflate the global decomposition rate by 1.7 times. Therefore, future litter decomposition studies should incubate separately fine roots by orders or functions (i.e., absorptive vs transportive), and separate them from rhizomes and leaves to be accurate. It is also critical to determine decomposition, lifespans and production rates[47] for all litter types in salt marshes (most of those data are currently lacking) to accurately identify and quantify organic matter inputs to salt marsh sediments.

In addition, most of the belowground decomposition rates (~90%[54]) are based on decomposition studies that combine all root functional types, even often excluding fine absorptive roots. Yet, we show that the belowground litter pool is not uniform in salt marshes as previously reported for terrestrial soils[24,36,37], with fine absorptive roots losing the least amount of C during decomposition in both ecosystems. Similar results have been found in mangroves[26], but so far, no such investigations in tropical and subtropical salt marshes. Our study suggests that in view of the importance of belowground litter for the C budget of Blue C ecosystems, differences in decomposition for contrasting root litter types should be taken into account when assessing litter decomposition in these ecosystems.

Further efforts, should consider processes of OM stabilization in sediments, such as the association of OM with minerals[55]. Indeed, the litter is first broken down into simpler compounds by microorganisms like bacteria, fungi, and other soil organisms. The decomposition process results in a processing of most of the litter inputs to the soil[55]. The remaining litter then undergoes process of stabilization and our study does not encompass this phase[55].

Conclusion

- The OM decomposition rate and quality were modulated by litter types with fine absorptive roots showing the lowest decomposition rate (up to 50% slower), followed by rhizomes, fine transportive roots and leaves. Consequently, rough global estimates based on aboveground

litter as a whole pool may likely overestimate the total litter decomposition rate.
- Elemental ratios (C:N) and concentrations (% N) failed to explain the difference in decomposition rate across the litter types, which were better explained by the composition of the different litter types, in particular by their lignin composition.
- The increase in inundation from the initial condition did not reduce the litter decomposition rate (except between extremes). This suggests that a gain in elevation through soil accretion is unlikely to result from a reduction in litter decomposition with an increase in inundation.

Methods

Field site

The in-situ manipulative experiment was conducted in a temperate salt marsh (Bossys perdus) in France between May and October 2021. Bossys perdus is situated within the maritime part of the Lilleau des Niges national biosphere reserve on Ré Island (French Atlantic Coast, Fig. 4) (46°13'42.4"N, 1°30'09.5"W). The dominant species in our experimental unit was *Halimione portulacoides*, a perennial C3 halophyte (angiosperm) that covers ~70% of the low vegetated area (Fig. 4)[56]. *Halimione portulacoides* belongs to the chenopod family. The climate of Bossys perdus is temperate oceanic with mild winters and warm summers. The mean annual precipitation is 744 mm, and the mean annual temperature is 13.3 °C[56]. The tidal regime is macro-tidal with spring tides reaching up to ~3.5 m in height[56]. Bossys perdus is flooded twice a day (semi-diurnal tides) with tidal waters from the Breton Sound mixed with inland waters from two rivers (Sèvre Niortaise and the Lay) and the upstream brackish marsh. The water salinity is around 32 ppt[56]. The sediments are dominated by silt (77%), followed by clay (12%) and sand (10%) at the surface and sand dominated in the deep sediment layers (unpublished results of Amann et al.). The total organic carbon content was 4% between the 0–10 cm depth in the sediment revealing the mostly minerogenic nature of our site (unpublished results of Amann et al.). The period of measurement in 2021 was typical of previous years in terms of tidal range at the site[56]. There were no periods of extreme sea levels at the studied site during our measurement periods from 2020 to 2022 and in 2021 after classical successive patterns of spring and ebbing tide periods along the years[56] (based also on unpublished measurements). Tidal waters immersed the site only during a quarter of time during flooding tides in spring and autumn[56]. Water height differences between 2020, 2021 (sampling period) and 2022 remained below 15 cm[56] (based also on unpublished measurements).

Experimental design of the marsh organ simulating an inundation gradient

We set up a marsh organ at Bossys perdus in April 2021. A marsh organ consists of mesocosm rows positioned at different elevations relative to the marsh surface to simulate a gradient of inundation duration and frequency[16,57]. The lower the mesocosm row, the longer the flooding duration and depth of the mesocosms is (Fig. 4). The potential impact of sea-level change on the inundation duration at Bossys perdus has not been fully established due to the lack of data on the root dynamics under accelerated SLR, which could potentially increase the soil elevation and thus reduce the inundation duration. Hence, we adopted a simplified approach without taking this feedback loop into account (Fig. 4)[12]. We designed five elevations: the first mesocosm row was set at an elevation of 130 cm, corresponding to the mean altitude of our site (referred to as "SLI"), and the mean inundation of our site. The second mesocosm row was positioned 30 cm lower than the SLI, simulating increased inundation resulting from the projected SLR under SSP1-2.6 (low emission scenarios)[58]. The third mesocosm row was placed 60 cm lower than the SLI, simulating increased inundation resulting from the projected SLR corresponding to the upper limit of the SSP3-7.0 (high emission scenarios)[58]. The fourth mesocosm row was established 100 cm lower than the SLI, simulating increased inundation resulting from the worst-case scenarios of SLR under SSP5-8.5. Lastly, a mesocosm row was placed 40 cm higher than the SLI to encompass a wide range of inundation durations (Fig. 4).

Each mesocosm consisted of a PVC tube closed at the bottom (20 cm diameter × 40 cm length) with a perforated lid for water drainage (Fig. 4). While marsh organ mesocosms are typically filled with reworked native sediments and transplanted with sods and seedlings, we used "intact" soil cores and in-situ grown vegetation directly from the site to closely simulate the environmental conditions (e.g., soil structure and drainage, microbial community, mature vegetation). We sharpened the ends of the mesocosms and used them as corers to randomly extract soil cores with intact *Halimione portulacoides* vegetation across the site. These soil cores were immediately placed in the marsh organ at the beginning of April 2021.

Experimental setup

We prepared 100 litterbags, including 25 filled with only leave litter, 25 only with fine absorptive root litter, 25 only with fine transportive root litter and 25 only with rhizomes litter. In each mesocosm, we buried 4 litterbags including one litterbag filled with leaf litter, one with fine absorptive root litter, one with fine transportive root litter and one with rhizome litter. We ensured that the litter collected from across our site was representative of our study area. We did not associate one location of litter collection to one mesocosm, because it could have potentially induced a confounding effect of litter location and quality. Our focus was on testing the effects of different litter types and inundation treatments, not on litter quality variations within the site due to location. Nevertheless, the litter heterogeneity across our collection points was likely minimal, as all the collected litter came from *Halimione portulacoide* plants situated between the edge of the marsh and 25 m inland, corresponding to a relatively small elevation gradient of less than 20 cm. The litter was extracted litter from 20 cores (15 cm length × 10 cm diameter) of soil and above-ground vegetation of *Halimione portulacoides* at the Bossys perdus site that were chosen randomly. *Halimione portulacoides* is prevalent as a mono-species in large areas of our site (Fig. 4). The belowground biomass of *Halimione portulacoides* is variable, ranging from 1151 to 6500 g dw m^{-2} across the seasons and salt marshes and

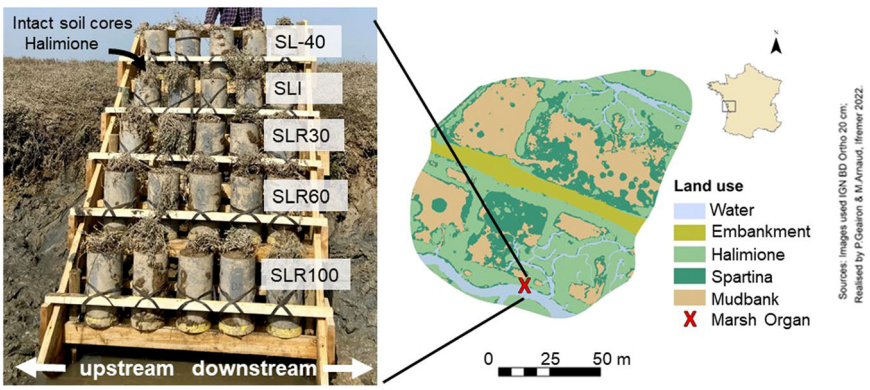

Fig. 4 | Marsh organ design and location of the Bossys perdus site. SLI is the initial level of inundation, SLR30, SLR60 and SLR100 are the inundation treatments corresponding to the projected SLR scenarios from low to above the worst-case emission scenarios[58]. For SL-40, the inundation duration was reduced compared to the mean inundation time (Table 1).

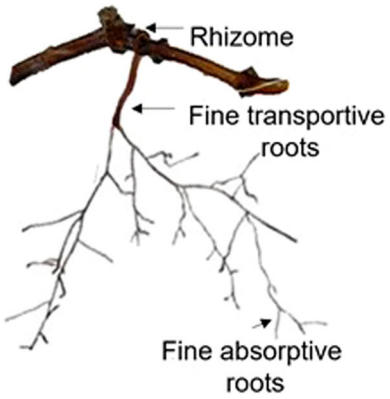

Fig. 5 | Diagram of the root functional types and rhizomes of *Halimione portulacoide* (not in scale).

representing up to 40% of the total biomass and 20% of the total mass of a soil core[59].

We extracted the soil core at least 2 m away from any other species, following the methods outlined by Freschet et al.[60]. To ensure species identity and root functional type identification, we only harvested *Halimione portulacoides* roots attached to the stem or rhizomes from the soil cores (note that there were no other species in our core)[60]. We then sorted the roots into functional types, including fine absorptive roots (root orders 1 and 2), fine transportive roots (root order 4) and rhizomes (Fig. 5)[60]. Due to coring restrictions in the biosphere reserve, we also directly collected fine absorptive roots, fine transportive roots and rhizomes attached to the stems or rhizomes of *Halimione portulacoides* from the 0 to 10 cm soil horizon at the Bossys perdus. Then, all of the roots and rhizomes were washed with water through a 1 mm sieve. We collected *Halimione portulacoides* leaves from the same area at the same time. All of the litter materials were dried at 40 °C in an oven for 4 days (i.e., until constant weight)[25,60].

We weighed 3 ± 0.05 g of each of the dry litter materials using a high-precision balance (±0.001 g, Sartorius, model no. 1712001, Germany) and filled the litterbags (7 cm in length, 5 cm in width and 0.45 µm mesh size) with the two functional root types, rhizomes and leaves separately and then buried them at a depth of 0.5 cm in each mesocosm. In each mesocosm, we buried four litter bags having one type of litter each. The litterbags were placed vertically in the sediments, and were not thick (<1 cm), so there was plenty of space between the litter bags and the mesocosms edge. We aimed to compare the decomposition of the different litter types under the same environmental conditions; therefore, we applied the exact same conditions for all litter types to avoid any confounding variations. This pooling has been reported as important to "ensure there are no biases in root properties, for example, in relation to collection depth or edaphic conditions"[34].

In total, we had four types of litter crossed with inundation treatments, each replicated five times, resulting in a total of 100 litterbags, which were buried in the 25 mesocosms for 170 days (May 4, 2021–October 21, 2021). Our incubation time was limited and only represents the first phase of OM decomposition. After excavation, the litterbags were individually washed, dried at 40 °C in an oven for 4 days, weighed (±0.001 g, Sartorius, model no. 1712001, Germany), and visually checked for defects. Two of the litterbags were damaged during the excavation and therefore have been removed from the analysis. Here, we define decomposition as all biological processes contributing to organic matter (OM) mass loss and transformation, in addition to leaching from litter only[61], and not consider stabilization processes that occurs in later phase. Hereafter, when we refer to OM, it is specifically OM derived from litter.

Carbon-Nitrogen and isotopic analysis

The C and N contents (% of organic C and % N) and the stable C and N isotope composition ($\delta^{13}C$ and $\delta^{15}N$) of the leaves, rhizomes and root materials were determined before and after field exposure (i.e., on decomposing litter). C, N, $\delta^{13}C$ and $\delta^{15}N$ were measured using a continuous flow Elementar® VarioPyro cube elemental analyzer (Elementar, Germany) coupled to a Micromass® Isoprime Isotope Ratio mass spectrometer (IRMS).

Pyrolysis coupled with gas chromatography and mass spectroscopy

Pyrolysis combined with gas chromatography-mass spectrometry (Py-GC/MS) provides a molecular fingerprint of the pyrolysable OM (i.e., the fraction of OM released as volatile compounds during pyrolysis and analyzed by GC/MS). Py-GC/MS allows for a qualitative characterization of the OM. Here, we used Py-GC/MS to determine the chemical structure of each litter type, as well as their decomposition proxies, including the lignin (Lig) to polysaccharide (PS) ratio and the syringyl lignin (LigS) to guaiacyl lignin (LigG) ratio (Thevenot et al., 2010) for litter types containing lignin (e.g., roots and rhizomes). Note that it was not possible to estimate the ratio for the leaves because they contain too little lignin. In summary, approximately 0.5 to 1 mg of each litter type was loaded into quartz tubes, which were then inserted into a pyrolysis unit (CDS Pyroprobe 5000 series, JSB, USA) and rapidly heated by a resistance heater to 650 °C within 0.15 sec (with a 30-s hold). The resulting pyrolysis products were separated using an Agilent 5890 gas chromatograph (GC) (Agilent Technologies, USA) coupled to a quadrupole mass spectrometer (Agilent 5889) operating in electron ionization mode (70 eV). Compounds were identified based on their mass spectra, GC retention times and comparison with library mass spectra (Wiley Library). Several pyrolysis products were identified for each sample, some of which were specific to a particular macromolecular source. The peaks were integrated using the ChemStation software (version D.03.00.611) (Agilent Technologies, USA). The relative area was calculated for each peak by normalizing its area by the sum of the areas of all the identified peaks. For this analysis, we had one true replicate and three analytical replicates because this method is highly labor-intensive in terms of data processing.

Environmental data collection

We measured the volumetric water content of the soil using an ML3 ThetaProbe (±1%, DeltaT Devices; Cambridge, UK) across all of the mesocosms at four random times ($n = 100$). The ML3 ThetaProbe measures the volumetric water content in a cylinder of sediment 3 cm in diameter and 6 cm in length. The inundation duration was determined from the water level height measured every 10 min using a multi-parameter probe STPS100SI (accuracy of the pressure sensor ±2.4 cm, NKE Instrumentation Ltd., France), between May 4, 2021 and October 20, 2021 at the level of the marsh organ. The precipitation was quantified every 10 min using a tipping bucket rain gauge (total accumulation in mm over each 10 min) (accuracy ± 5%, TE525MM, Texas Electronics, USA). The air temperature (°C) and the relative humidity (%) were measured every 10 min using an HMP155A probe (accuracy RH ± 1.7% Ta ± 0.055 °C, Campbell Scientific Ltd., UK). All of these meteorological parameters were measured at a single point on the site between May 4, 2021 and October 12, 2021 from an atmospheric Eddy Covariance station (Mayen et al., 2023). The soil temperature was measured using thermocouples (TE-C0010109-WIRE-010, Thermo-Electric, USA) at three points across the sites between July 26, 2021 and October 20, 2021.

Calculations and statistical analysis

We calculated the initial mass of carbon (C_Mass_initial in g) by multiplying the percentage of carbon content in the initial litter by the weight of the initial sample. A similar calculation was performed for the mass of carbon in the decomposing litter (C_Mass_final in g). We then determined the percentage of carbon loss relative to the initial carbon mass (the percentage change in %) using the following formula:

C percent change = 100 * ((C_Mass_initial - C_Mass_final) / C_Mass_initial))

The same procedure was applied for nitrogen (N). Similarly, we computed the percentage change for each decomposition proxy (without

calculating the mass, due to the qualitative values obtained from pyrolysis). We determined the percentage of change to normalize the change of each variable compared to their initial value. To process our results, we conducted a Principal Component Analysis (PCA) to summarize the pyrolysis results by attributing the main molecules that constitute each litter type using the "ade4" R package[62]. We used linear model to investigate the effect of the litter types, inundation treatments and their two-way interaction on the OM decomposition rate over 170 days. The fixed factors were the inundation level and the litter types. We conducted Tukey post-hoc comparisons between the least-square means for all pairs of samples. Visual inspection of the linear model residuals did not reveal any deviations from normality, homoscedasticity or linearity. The residuals of the linear model did not show any hierarchical structure. We determined the effects of litter types, inundation treatment and their interaction for the other variables (C, N, $\delta^{13}C$, $\delta^{15}N$, Lig:PS, LigS:LigG) using two-way ANOVAs or Kruskal-Wallis tests if the ANOVA assumption was not met. Post-hoc pairwise comparisons were conducted using Tukey's HSD tests following the ANOVA test, and the Dunn test was used after the Kruskal-Wallis test. We visually inspected the residuals, and there were no obvious deviations from normality or homoscedasticity for the ANOVAs. We did a linear regression between mass loss and inundation as a continuous variable (as h d^{-1}). We used R to perform all of the statistical analyses, including the R package stats[63].

Limitations of the experimental design

We purposefully did not associate one plant from one location to one mesocosm, as this could have potentially introduced a confounding effect of litter quality due to location. The approach of using standardized material or pooled materials in decomposition studies has been highly recommended in methodological papers to avoid such biases[34,42] and has been employed in many decomposition studies in saltmarshes[54] and in studies comparing different types of litter. Nevertheless, this approach reduces the variability across replicates, and this should be kept in mind when interpreting our results. The use of litterbags with a small mesh size allowed for OM decomposition by microbes, fungi and microfauna, but excluded decomposers larger than 0.45 µm (i.e., meso and meiofauna). The use of a small mesh size was necessary to prevent litterbag contamination from new root materials growing within the litterbags. In addition, as in any experiment, we reduced the complexity of the system using mesocosms (e.g., isolation of the mesocosms from other habitats), even though our mesocosms have been filled with intact soil cores randomly selected from the salt marsh location and which were notably larger compared to most previous marsh organ studies[16,17]. Our litter was dried at a low temperature to avoid altering the litter chemistry, following the recommendation of Freschet et al. (2021)[60]. Drying is commonly performed in litterbag studies to compare leaves and root functional types[25,60] and is necessary since using a wet-dry mass ratio may lead to significant errors in the final mass losses. We chose a single sampling date due to the logistical challenge of collecting additional fine absorptive roots for extra litterbags (without freezing the roots), as it is an extremely time-consuming process to collect and sort roots. Nevertheless, our incubation occurred during the most active months for decomposition, and a single sampling time was sufficient to address our research questions. Our incubation time was limited and only represents the first phase of OM decomposition. Also, we studied only the litter decomposition that only partially control the C input to salt marsh sediments. The impact of shading on soil temperature may also affect litter decomposition in the experiments. To mitigate shading effects and ensure consistent sunlight exposure for each row, we positioned the elevation platform so that it faced southward[50]. Lastly, we measured the OM decomposition rate only and not loss through erosion, while SLR can lead to an increase of salt marsh erosion, and thus loss of OM[9]. These differences between our mesocosm and the natural system should be kept in mind when interpreting our results.

Data availability

The data that support the findings of this study are available in the Supplementary Data 1 of this article and in a Zenodo repository[64].

Received: 18 December 2023; Accepted: 30 October 2024;
Published online: 09 November 2024

References

1. McLeod, E. et al. A blueprint for blue carbon: toward an improved understanding of the role of vegetated coastal habitats in sequestering CO_2. *Front. Ecol. Environ.* **9**, 552–560 (2011).
2. Macreadie, P. I. et al. Blue carbon as a natural climate solution. *Nat. Rev. Earth Environ.* **2**, 826–839 (2021).
3. Van De Broek, M. et al. Long-term organic carbon sequestration in tidal marsh sediments is dominated by old-aged allochthonous inputs in a macrotidal estuary. *Glob. Change Biol.* **24**, 2498–2512 (2018).
4. Alongi, D. M. Carbon balance in salt marsh and mangrove ecosystems: a global synthesis. *J. Mar. Sci. Eng.* **8**, 767 (2020).
5. Spivak, A. C., Sanderman, J., Bowen, J. L., Canuel, E. A. & Hopkinson, C. S. Global-change controls on soil-carbon accumulation and loss in coastal vegetated ecosystems. *Nat. Geosci.* **12**, 685–692 (2019).
6. Schuerch, M. et al. Future response of global coastal wetlands to sea-level rise. *Nature* **561**, 231–234 (2018).
7. Rogers, K. et al. Wetland carbon storage controlled by millennial-scale variation in relative sea-level rise. *Nature* **567**, 91–95 (2019).
8. Zhu, C., Langley, J. A., Ziska, L. H., Cahoon, D. R. & Megonigal, J. P. Accelerated sea-level rise is suppressing CO_2 stimulation of tidal marsh productivity: A 33-year study. *Sci. Adv.* **8**, eabn0054 (2022).
9. Valiela, I. et al. Transient coastal landscapes: Rising sea level threatens salt marshes. *Sci. Total Environ.* **640**, 1148–1156 (2018).
10. Megonigal, J. P., Hines, M. E. & Visscher, P. T. *Anaerobic metabolism: linkages to trace gases and aerobic processes*. in *Treatise on Geochemistry* 317–424 (Elsevier, 2003). https://doi.org/10.1016/B0-08-043751-6/08132-9.
11. Davidson, E. A. & Janssens, I. A. Temperature sensitivity of soil carbon decomposition and feedbacks to climate change. *Nature* **440**, 165–173 (2006).
12. Arnaud, M., Baird, A. J., Morris, P. J., Dang, T. H. & Nguyen, T. T. Sensitivity of mangrove soil organic matter decay to warming and sea level change. *Glob. Change Biol.* **26**, 1899–1907 (2020).
13. Wang, F., Kroeger, K. D., Gonneea, M. E., Pohlman, J. W. & Tang, J. Water salinity and inundation control soil carbon decomposition during salt marsh restoration: an incubation experiment. *Ecol. Evol.* **9**, 1911–1921 (2019).
14. Mueller, P., Jensen, K. & Megonigal, J. P. Plants mediate soil organic matter decomposition in response to sea level rise. *Glob. Change Biol.* **22**, 404–414 (2016).
15. Morrissey, E. M., Gillespie, J. L., Morina, J. C. & Franklin, R. B. Salinity affects microbial activity and soil organic matter content in tidal wetlands. *Glob. Change Biol.* **20**, 1351–1362 (2014).
16. Kirwan, M. L., Langley, J. A., Guntenspergen, G. R. & Megonigal, J. P. The impact of sea-level rise on organic matter decay rates in Chesapeake Bay brackish tidal marshes. *Biogeosciences* **10**, 1869–1876 (2013).
17. Janousek, C. N. et al. Inundation, vegetation, and sediment effects on litter decomposition in Pacific Coast Tidal Marshes. *Ecosystems* **20**, 1296–1310 (2017).
18. Mueller, P. et al. Global-change effects on early-stage decomposition processes in tidal wetlands – implications from a global survey using standardized litter. *Biogeosciences* **15**, 3189–3202 (2018).
19. Ouyang, X. et al. Response of macrophyte litter decomposition in global blue carbon ecosystems to climate change. *Glob. Change Biol.* **29**, 3806–3820 (2023).
20. McCormack, M. L. et al. Redefining fine roots improves understanding of below-ground contributions to terrestrial biosphere processes. *N. Phytol.* **207**, 505–518 (2015).
21. Beidler, K. V. & Pritchard, S. G. Maintaining connectivity: understanding the role of root order and mycelial networks in fine root decomposition of woody plants. *Plant Soil* **420**, 19–36 (2017).

22. Wang, G., Xue, S., Liu, F. & Liu, G. Nitrogen addition increases the production and turnover of the lower-order roots but not of the higher-order roots of Bothriochloa ischaemum. *Plant Soil* **415**, 423–434 (2017).
23. Silver, W. L. & Miya, R. K. Global patterns in root decomposition: Comparisons of climate and litter quality effects. *Oecologia* **129**, 407–419 (2001).
24. Fan, P. & Guo, D. Slow decomposition of lower order roots: a key mechanism of root carbon and nutrient retention in the soil. *Oecologia* **163**, 509–515 (2010).
25. Sun, T. et al. Early stage fine-root decomposition and its relationship with root order and soil depth in a Larix gmelinii plantation. *Proc. Natl Acad. Sci. USA* **115**, 10392–10397 (2018).
26. Zhang, Y. et al. The role of mangrove fine root production and decomposition on soil organic carbon component ratios. *Ecol. Indic.* **125**, 107525 (2021).
27. Yang, Z. et al. Differential responses of litter decomposition to regional excessive nitrogen input and global warming between two mangrove species. *Estuar. Coast. Shelf Sci.* **214**, 141–148 (2018).
28. Kelleway, J. J., Trevathan-Tackett, S. M., Baldock, J. & Critchley, L. P. Plant litter composition and stable isotope signatures vary during decomposition in blue carbon ecosystems. *Biogeochemistry* **158**, 147–165 (2022).
29. Benner, R., Fogel, M. L., Sprague, E. K. & Hodson, R. E. Depletion of 13C in lignin and its implications for stable carbon isotope studies. *Nature* **329**, 708–710 (1987).
30. Lanari, M., Coelho Claudino, M., Miranda Garcia, A. & Da Silva Copertino, M. Changes in the elemental (C, N) and isotopic (δ13C, δ15N) composition of estuarine plants during diagenesis and implications for ecological studies. *J. Exp. Mar. Biol. Ecol.* **500**, 46–54 (2018).
31. Thevenot, M., Dignac, M.-F. & Rumpel, C. Fate of lignins in soils: a review. *Soil Biol. Biochem.* **42**, 1200–1211 (2010).
32. Bi, W., Wang, J. J., Dodla, S. K., Gaston, L. A. & DeLaune, R. D. Lignin chemistry of wetland soil profiles in two contrasting basins of the Louisiana Gulf coast. *Org. Geochem.* **137**, 103902 (2019).
33. Redondo-Gomez, S. et al. Growth and photosynthetic responses to salinity of the salt-marsh shrub Atriplex portulacoides. *Ann. Bot.* **100**, 555–563 (2007).
34. Halbritter, A. H. et al. The handbook for standardized field and laboratory measurements in terrestrial climate change experiments and observational studies (ClimEx). *Methods Ecol. Evol.* **11**, 22–37 (2020).
35. Carrasco-Barea, L., Llorens, L., Romaní, A. M., Gispert, M. & Verdaguer, D. Litter decomposition of three halophytes in a Mediterranean salt marsh: Relevance of litter quality, microbial activity and microhabitat. *Sci. Total Environ.* **838**, 155743 (2022).
36. Goebel, M. et al. Decomposition of the finest root branching orders: Linking belowground dynamics to fine-root function and structure. *Ecol. Monogr.* **81**, 89–102 (2011).
37. Xiong, Y. et al. Fine root functional group based estimates of fine root production and turnover rate in natural mangrove forests. *Plant Soil* **413**, 83–95 (2013).
38. Hemminga, M. A. & Buth, G. J. C. Decomposition in Salt Marsh Ecosystems of the S.W. Netherlands: the effects of biotic and abiotic factors. *Vegetation* **92**, 73–83 (1991).
39. Keiluweit, M., Nico, P. S., Kleber, M. & Fendorf, S. Are oxygen limitations under recognized regulators of organic carbon turnover in upland soils? *Biogeochemistry* **127**, 157–171 (2016).
40. Bahri, H. et al. Lignin degradation during a laboratory incubation followed by 13C isotope analysis. *Soil Biol. Biochem.* **40**, 1916–1922 (2008).
41. Talbot, J. M., Yelle, D. J., Nowick, J. & Treseder, K. K. Litter decay rates are determined by lignin chemistry. *Biogeochemistry* **108**, 279–295 (2012).
42. Keuskamp, J. A., Dingemans, B. J. J., Lehtinen, T., Sarneel, J. M. & Hefting, M. M. Tea Bag Index: a novel approach to collect uniform decomposition data across ecosystems. *Methods Ecol. Evol.* **4**, 1070–1075 (2013).
43. Lewis, D. B., Brown, J. A. & Jimenez, K. L. Effects of flooding and warming on soil organic matter mineralization in Avicennia germinans mangrove forests and Juncus roemerianus salt marshes. *Estuar. Coast. Shelf Sci.* **139**, 11–19 (2014).
44. Liu, B. et al. Interactive effects of sea-level rise and nitrogen enrichment on the decay of different plant residues in an oligohaline estuarine marsh. *Estuar. Coast. Shelf Sci.* **270**, 107835 (2022).
45. Aller, R. C. Bioturbation and remineralization of sedimentary organic matter: effects of redox oscillation. *Chem. Geol.* **114**, 331–345 (1994).
46. Reimers, C. E. et al. Redox effects on the microbial degradation of refractory organic matter in marine sediments. *Geochim. et. Cosmochim. Acta* **121**, 582–598 (2013).
47. Arnaud, M. et al. Global mangrove root production, its controls and roles in the blue carbon budget of mangroves. *Glob. Change Biol.* **29**, 3256–3270 (2023).
48. Kirwan, M. L. & Megonigal, J. P. Tidal wetland stability in the face of human impacts and sea-level rise. *Nature* **504**, 53–60 (2013).
49. De Battisti, D. et al. Multiple trait dimensions mediate stress gradient effects on plant biomass allocation, with implications for coastal ecosystem services. *J. Ecol.* **108**, 1227–1240 (2020).
50. Kirwan, M. L. & Guntenspergen, G. R. Feedbacks between inundation, root production, and shoot growth in a rapidly submerging brackish marsh. *J. Ecol.* **100**, 764–770 (2012).
51. Allen, J. Morphodynamics of Holocene salt marshes: a review sketch from the Atlantic and Southern North Sea coasts of Europe. *Quat. Sci. Rev.* **19**, 1155–1231 (2000).
52. Reef, R. et al. The effects of CO2 and nutrient fertilisation on the growth and temperature response of the mangrove Avicennia germinans. *Photosynthesis Res.* **129**, 159–170 (2016).
53. Kirwan, M. L., Temmerman, S., Skeehan, E. E., Guntenspergen, G. R. & Fagherazzi, S. Overestimation of marsh vulnerability to sea level rise. *Nat. Clim. Change* **6**, 253–260 (2016).
54. Ouyang, X., Lee, S. Y. & Connolly, R. M. The role of root decomposition in global mangrove and saltmarsh carbon budgets. *Earth-Sci. Rev.* **166**, 53–63 (2017).
55. Prescott, C. E. Litter decomposition: what controls it and how can we alter it to sequester more carbon in forest soils? *Biogeochemistry* **101**, 133–149 (2010).
56. Mayen, J. et al. Atmospheric CO_2 exchanges measured by eddy covariance over a temperate salt marsh and influence of environmental controlling factors. *Biogeosciences* **21**, 993–1016 (2024).
57. Morris, J. T. Estimating net primary production of salt marsh macrophytes. in *Principles and Standards for Measuring Primary Production* (eds. Fahey, T. J. & Knapp, A. K.) 106–119 (Oxford University Press, 2007). https://doi.org/10.1093/acprof:oso/9780195168662.003.0007.
58. IPCC. Climate Change 2021: The Physical Science Basis. Contribution of Working Group I to the Sixth Assessment Report of the Intergovernmental Panel on Climate Change (eds. Masson-Delmotte, V. et al.) (Cambridge, 2021).
59. Caçador, I., Vale, C. & Catarino, F. Seasonal variation of Zn, Pb, Cu and Cd concentrations in the root–sediment system of Spartina maritima and Halimione portulacoides from Tagus estuary salt marshes. *Mar. Environ. Res.* **49**, 279–290 (2000).
60. Freschet, G. T. et al. A starting guide to root ecology: strengthening ecological concepts and standardising root classification, sampling, processing and trait measurements. *N. Phytol.* **232**, 973–1122 (2021).
61. Couteaux, M.-M., Bottner, P. & Berg, B. Litter decomposition, climate and liter quality. *Trends Ecol. Evol.* **10**, 63–66 (1995).
62. Dray, S. & Dufour, A.-B. The **ade4** Package: implementing the duality diagram for ecologists. *J. Stat. Soft*. **22**, 1–20 (2007).

63. Core Team, R. R: A language and environment for statistical computing. R Foundation for Statistical Computing (2021).
64. Arnaud, M. et al. Salt marsh litter quality and decomposition under sea-level rise scenarios: from leaves to fine absorptive roots. *EGU General Assembly*. https://doi.org/10.5194/egusphere-egu24-5879 (2024).

Acknowledgements

Funding for this project has been received from an individual post-doctoral fellowship from Ifremer (Scientific Direction) awarded to M.A., and from a Master's student grant from the CNRS awarded to M.B. The ANR project PAMPAS (ANR-18-CE32-0006) and the LEFE project DYCIDEMAIM (DEC21069DR16) are linked to the post-doc project. DYCIDEMAIM paid the fieldwork expenses. The chemical analyses were funded by the CNRS. We thank the management board of Lilleau des Niges and the LPO for giving us authorization to access the site and for their support (including from the volunteers). We thank P. and J.Y. Baraton for their support during the fieldwork. We thank INRAe Bordeaux for the supply of soil instrumentation and help during the fieldwork.

Author contributions

M.A. and P.P. designed the study with C.R. and M.F.D. inputs. M.A. lead the analysis of the results and the writing of the manuscript with inputs of M.B., C.R., M.F.D., N.B., R.J.N., J.D., P.G., P.K., J.G., J.C.L., M.A., M.B. performed field and laboratory analysis with help of P.P., C.R., M.F.D., N.B., R.J.N., J.D., P.G., P.K., J.G., J.C.L.

Competing interests

The authors declare no competing interests.

Additional information

Supplementary information The online version contains supplementary material available at https://doi.org/10.1038/s43247-024-01855-0.

Correspondence and requests for materials should be addressed to Marie Arnaud.

Peer review information *Communications Earth and Environment* thanks Vanessa Wong and the other, anonymous, reviewer(s) for their contribution to the peer review of this work. Primary Handling Editors: Nadine Schubert, Joe Aslin and Clare Davis. A peer review file is available.